

# Continual Learning with Dynamic Sparse Training: Exploring Algorithms for Effective Model Updates

Murat Onur Yildirim<sup>1</sup>, Elif Ceren Gok Yildirim<sup>1</sup>, Ghada Sokar<sup>1</sup>, Decebal Constantin Mocanu<sup>2</sup>, Joaquin Vanschoren<sup>1</sup>

<sup>1</sup>Eindhoven University of Technology, <sup>2</sup>University of Luxembourg  
m.o.yildirim@tue.nl, e.c.gok@tue.nl, g.a.z.n.sokar@tue.nl,  
decebal.mocanu@uni.lu, j.vanschoren@tue.nl

Continual learning (CL) refers to the ability of an intelligent system to sequentially acquire and retain knowledge from a stream of data with as little computational overhead as possible. To this end; regularization, replay, architecture, and parameter isolation approaches were introduced to the literature. Parameter isolation using a sparse network which enables to allocate distinct parts of the neural network to different tasks and also allows to share of parameters between tasks if they are similar. Dynamic Sparse Training (DST) is a prominent way to find these sparse networks and isolate them for each task. This paper is the first empirical study investigating the effect of different DST components under the CL paradigm to fill a critical research gap and shed light on the optimal configuration of DST for CL if it exists. Therefore, we perform a comprehensive study in which we investigate various DST components to find the best topology per task on well-known CIFAR100 and miniImageNet benchmarks in a task-incremental CL setup since our primary focus is to evaluate the performance of various DST criteria, rather than the process of mask selection. We found that, at a low sparsity level, Erdős-Rényi Kernel (ERK) initialization utilizes the backbone more efficiently and allows to effectively learn increments of tasks. At a high sparsity level, however, uniform initialization demonstrates more reliable and robust performance. In terms of growth strategy; performance is dependent on the defined initialization strategy, and the extent of sparsity. Finally, adaptivity within DST components is a promising way for better continual learners.

## 1. Introduction

Continual learning (CL) is a method of developing models that can learn and adapt continuously from a stream of data, or tasks, unlike the standard batch learning that necessitates access to all categories' data simultaneously. Therefore, it allows efficient learning and avoids the storage of large amounts of data. However, this often comes at a price, known as *catastrophic forgetting*, the degradation of previously learned information as the deep learner focuses on learning new ones. Four major approaches have been explored to address this issue. Regularization [1–5] prevents abrupt changes in the neural network weights. Replay stores a few real exemplars [6–8] or generates some synthetic exemplars by learning the data distribution [9–12] per class and rehearses them. Architecture expansion [13–17] modifies the network architecture, typically by adding extra network components. Parameter isolation [18–27] partitions the neural network into subnetworks that are dedicated to different tasks and freezes the weights of subnetworks which allows to preserve previously learned knowledge. In this paper, we focus on the parameter isolation approach due to its fixed network capacity usage, low tendency to forget, and its memory- and computation-wise efficiency.

Parameter isolation typically freezes the connections of previous subnetworks and only updates newly added ones to be able to learn the current subnetwork. It can be performed via mask learning [18, 19], iterative pruning [20–22] or dynamic sparse training (DST) [23–27]. Mask learning utilizes a fixed, usually pre-trained, dense backbone and only intends to find the best mask for a given task. Iterative pruning trains a dense network and then iteratively removes the unpromising weights with a smallest magnitude whereas DST aims to train sparse network from scratch and find the best topology simultaneously by dropping and growing different components of the network during training to discover the best sparse topology. It reduces the number of

parameters quadratically during both training and inference without compromising the accuracy [28]. DST can be performed on neuron-level or connection-level which are known as structured and unstructured pruning respectively. Although structured pruning allows computationally more efficient subnetworks, it has been shown to perform less compared to unstructured pruning on higher sparsity levels [29] which reserves more space for subsequent tasks in the network.

In this paper, we conducted large-scale experiments on CIFAR100 and miniImageNet with a different number of tasks. We analyze unstructured DST performance in CL in terms of incremental accuracy, backward, and forward transfer under various sparsity levels, initializations, and growth strategies. We focus on task-incremental CL since we specifically want to observe the performance of different DST criteria, not the process of mask selection. Our findings are:

- I. At a low to moderate sparsity level, Erdős-Rényi Kernel (ERK) initialization utilizes the backbone more efficiently by using the connections within the narrow layers sparingly which allows to effectively learn increments of tasks.
- II. At a high sparsity level, uniform initialization demonstrates more robust incremental performance by maintaining stable performance over tasks.
- III. From the growth strategy standpoint, performance outcomes are dependent on defined initialization strategy, and the degree of sparsity.
- IV. Selecting the DST criteria adaptively per task holds a promise to significantly enhance the incremental performance of a model, compared to the pre-defined strategies for all tasks. We show that even a naive alteration between different growth strategies boosts incremental performance.

## 2. Background and Related Work

**DST for Standard Batch Learning.** Dynamic sparse training is a technique to attain a sparse network in which the model is initialized with a random sparse topology and then the connections are dynamically pruned and grown during the training process to improve computational efficiency and generalization performance [28]. This involves an update period of the network topology and a drop/growth strategy to explore the network within a pre-defined sparsity level while minimizing the loss function by preserving important weights for a given task. By reducing the number of connections, dynamic sparse training can speed up training and reduce memory requirements while maintaining or even improving model accuracy [30].

SET [28] is the pioneer study of DST and discovers an optimal sparse connectivity pattern during training by introducing *Erdős-Rényi* (ER) initialization and random growth. ER initialization assigns more connections to smaller layers while allocating fewer connections to the large ones in MultiLayer Perceptrons (MLPs) with  $\frac{\epsilon(n^{l-1}+n^l)}{n^{l-1}n^l}$  where  $n^l$  denotes the number of neurons at layer  $l$  and  $\epsilon$  indicates the sparsity level. Random growth randomly connects an equal number of weights that are dropped based on their *magnitudes* to explore a new sparse topology. Inspired by SET, RigL [31] and SNFS [32] introduced gradient growth and momentum growth: the idea of using gradient and momentum information obtained by backward pass is to grow the promising connections that accelerate the exploration of optimal sparse topology. Although gradient and momentum growth accelerate the exploration of optimal sparse topology, they require a dense backward pass to use the information of both existing and the non-existing connections. To improve this, Top-KAST [33] opted to use the gradients corresponding to a subset of the non-existent connections. Furthermore, [34, 35] thoroughly study the dynamic sparse training and sparse topologies, and found that the performance of the sparse networks can outperform the dense counterparts.

**DST for Continual Learning.** Prior work [36] showed that dynamically shrinking and expanding the model capacity effectively avoids the excessive pruning, compared to the iterative pruning over sequential tasks. Hence, Dynamic Sparse Training is a viable Parameter Isolation approach for Continual Learning since it can assign specific components to different tasks while exploring the network with different topologies. SpaceNet [23] and AFAF [24] opt to utilize DST in a structured manner that explores the best sparse topology on a neuron-level whereas NISPA [25], WSN [26] and SparCL [27] perform it in an unstructured manner which is a connection-level search. SpaceNet allows having limited common units among subnetworks to

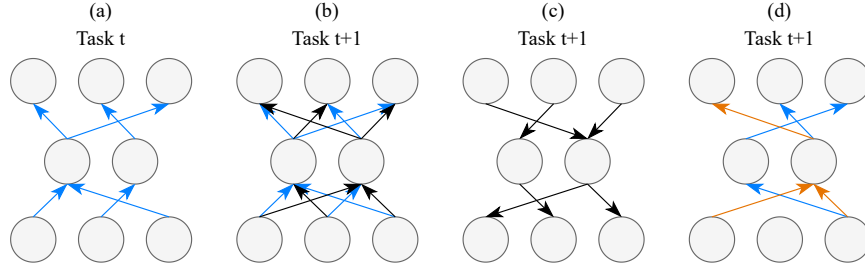


Figure 1: Illustration of Continual DST. (a) **Learned connections** for Task  $t$ , (b) in the forward pass of a new task, the model is free to use all the connections, (c) yet in the backward pass it is only allowed to update the **unassigned connections**, (d) after dynamically exploring the network with steps (b) and (c) under a sparsity level of  $s\%$ , subsequent subnetworks which can include **new connections** and previously **learned connections** are obtained.

prevent interference between tasks while NISPA, WSN, and AFAF exploit units from previous subnetworks fully to utilize the backbone efficiently and also transfer the relevant knowledge. NISPA selects the candidate connections randomly while WSN chooses them based on the gradients. To enable practical on-device CL, SparCL integrates weight sparsity with data removal and gradient sparsity.

However, in CL scenarios, none of those studies have extensively explored the effect of different initialization, drop, and growth strategies which have a high influence on the final sparse neural network topology and performance.

### 3. Method

In this section, we give an overview of dynamic sparse training and its application in the context of continual learning. Specifically, we provide a Continual DST that focuses on adapting dynamic sparse training to the continual learning setting, where the goal is to learn and retain knowledge from a sequence of tasks without catastrophic forgetting. We present the underlying formulation and optimization objectives that guide our exploration of hyperparameters and design choices within this framework.

**Overview.** As shown in Figure 1, Continual DST starts with an over-parameterized neural network in which we searched for the task-specific subnetworks and only changed the weights that are not trained on the previous tasks. In other words, we froze the parameters of the selected subnetwork after training to prevent catastrophic forgetting yet we allowed to use those frozen parameters in the subsequent tasks. This supports the transfer of previous knowledge to future tasks, also known as forward transfer. It is particularly important for large-scale continual learning problems as it decreases the time required to converge during sequential learning.

**Continual DST.** Continual learning involves updating a neural network with a sequence of learning tasks  $\mathcal{T}_{1:t} = (\mathcal{T}_1, \mathcal{T}_2, \dots, \mathcal{T}_t)$ , each with a corresponding dataset  $\mathcal{D}_{\mathcal{T}} = (x_{i,t}, y_{i,t})^{n_t}$  consisting of  $n_t$  instances per task. Upon encountering a new learning task, a deep network optimized to map the input instance to the classifier space, denoted as  $f_{\Theta} : \mathcal{X}_t \rightarrow \mathcal{Y}_t$ , where  $\Theta$  stands for the parameters of the network. Note that, the learning tasks are mutually exclusive, i.e.,  $\mathcal{Y}_{t-1} \cap \mathcal{Y}_t = \emptyset$  and we assumed that task identity is given in both the training and the testing stage. The goal of Continual DST is to effectively learn the subnetwork by solving the optimization problem that minimizes the following function:

$$\mathcal{M}_t^* = \arg \min_{\mathcal{M}_t} \mathcal{L}(\Theta_s, n_t) = \arg \min_{\mathcal{M}_t} \sum_{i=1}^{n_t} [CE(f(x_{i,t}; \Theta_s), y_{i,t})] \quad (1)$$

Here,  $\mathcal{L}(\Theta_s, n_t)$  is the loss function, which is Cross-Entropy ( $CE$ ) in our experiments, with a pre-defined fraction of parameters  $\Theta_s$ , and by solving this optimization problem, mask  $\mathcal{M}_t$  is determined. Note that, although sparsity per task is predefined, the overall usage of the backbone is task-dependent and highly related to how much the tasks share the learned knowledge. Hence, overall sparsity on the backbone increases naturally yet sparsity per task will be the same for each task.

**Sparse Initialization.** We consider the following strategies for sparse initialization of the network.

*Uniform:* Sparsity of each layer, denoted as  $s$ , is equivalent to the overall network sparsity, represented by  $S$ .

*Erdős-Rényi Kernel (ERK)* [31]: Inspired by Erdős-Rényi initialization [28], ERK is formulated as  $\frac{\epsilon(n^{l-1}+n^l+w^l+h^l)}{n^{l-1}n^l w^l h^l}$  where  $\epsilon$  indicates the sparsity level,  $n^l$  denotes the number of neurons at layer  $l$ ,  $w^l$  and  $h^l$  are the width and the height of the  $l^{th}$  convolutional kernel. It allocates higher sparsities to the layers with more parameters and lower sparsities to the layers with fewer parameters while keeping the total sparsity at the level of  $S$ . The sparsity of the fully connected layers follows the same rules of the original Erdős-Rényi.

**Topology Update.** The topology update should balance *exploration vs. exploitation* trade-off to obtain better sparse topologies. The update schedule is determined by the following parameters: (1)  $\Delta T$ , the number of iterations between sparse connectivity updates (2)  $T_{end}$ , the iteration at which the sparse connectivity updates should be stopped (3)  $\alpha$ , the initial proportion of connections that are updated, and (4)  $f_{decay}$ , a function that is called every  $\Delta T$  iteration which gradually decreases the proportion of updated connections over time. Similar to the previous studies [25, 31, 32, 34], we use Cosine Annealing  $f_{decay}(t, \alpha, T_{end}) = \frac{\alpha}{2}(1 + \cos(\frac{t\pi}{T_{end}}))$  for topology update.

**Drop and Growth.** We consider the following drop and growth strategies to update the topology.

*Magnitude-based drop* [37]: It involves identifying and removing the connections with the lowest magnitudes or ‘saliency’ based on a predefined sparsity level or threshold.

*Random growth* [28]: It randomly adds new connections to the network and does not take into account any specific information about the network’s behavior or performance.

*Unfired growth:* It randomly adds new connections that have not been used or ‘fired’ before.

*Gradient growth* [31]: It involves adding new connections based on the gradients values of the connections during the training process. Connections with higher gradients or those that contribute more to the network’s error reduction are considered for growth.

*Momentum growth* [32]: It considers both the current gradient and the accumulated gradient from previous updates which smoothes out the updates over time. Connections with higher momentum are considered for growth since they are more promising to reduce the network’s error.

Gradient and momentum growth techniques are able to accelerate the search for an optimal subnetwork but they necessitate a dense backward pass that incorporates information from both existing and non-existing connections.

## 4. Experimental Setup

In this section, we briefly describe our experimental setup including the datasets used, the metrics employed for evaluation, and the implementation details that ensure the reproducibility and validity of our results.

**Datasets.** In this paper, we want to create scenarios with different numbers of tasks to see the impact of the DST strategies under various conditions. To this end, we experiment with CIFAR100 [38] and miniImageNet [39] which consist of objects from 100 different categories. We split CIFAR100 into 5, 10 and 20 distinct tasks with 20, 10 and 5 classes within each learning task and named them **5-task CIFAR100**, **10-task CIFAR100**, and **20-task CIFAR100** respectively. Finally, for a more challenging scenario, we use **10-task miniImageNet** in which the model learns 10 tasks with 10 classes within each incremental step.

**Metrics.** We resort to the well-known CL metrics for evaluation. **Accuracy (ACC)** [40] measures the final accuracy averaged over all tasks where  $A_{T,i}$  is the accuracy of task  $i$  after learning task  $T$ . **Backward transfer (BWT)** [40] measures the level of forgetting and the average accuracy change of each task after learning new tasks where  $A_{i,i}$  is the accuracy of task  $i$  just after learning task  $i$ . **Forward transfer (FWT)**, inspired from [40], measures the level of transfer where  $A_{j,i}$  is the accuracy of learned subnetwork on task  $i$  performing on task  $j$ , evaluates how well the model performs on the following tasks which are different from the tasks it was trained on.

$$ACC = \frac{1}{T} \sum_{i=1}^T A_{T,i} \quad (2)$$

$$BWT = \frac{1}{T-1} \sum_{i=1}^{T-1} (A_{T,i} - A_{i,i}) \quad (3)$$

$$FWT = \frac{1}{T-i} \sum_{i=1}^T \sum_{j=i+1}^T A_{j,i} \quad (4)$$

**Implementation Details.** We implement all the methods in PyTorch [41]. We use ResNet-18 [42] as the backbone for all datasets. We choose not to freeze batch normalizations during the training because they cannot be assigned as task-specific components. We have built on the ITOP library [34] which is developed for standard batch learning. We use Cosine Annealing for a drop rate starting from 0.5. We update the sparse topology after every 50, 100, 200, and 400 iterations. We set number of epochs to 25 for 20-task CIFAR100 whereas 100 for 5-task CIFAR100, 10-task CIFAR100 and 10-task miniImageNet. We use adam optimizer and set an initial learning rate of 0.001 which is decayed by a factor of 0.1 after 1/2 and 3/4 of the total number of epochs. We set the batch size to 128. We run experiments on three different seeds and report their average.

## 5. Results

In this section, we present the empirical analysis to investigate the effect of different DST components in a CL paradigm to understand the underlying mechanism and shed light on the optimal DST configuration for CL. We study on four distinct scenarios with different incremental steps and datasets which are 5-task CIFAR100, 10-task CIFAR100, 20-task CIFAR100, and 10-task miniImageNet to observe the effect of initialization, growth, and its adaptive selection between tasks.

### 5.1. Different initialization strategies require different sparsity levels.

In combination with various growth techniques and sparsity levels, initialization strategy significantly influences the incremental accuracy, especially when the number of tasks increases and tasks become more complex such as 10-Task miniImageNet, 10-Task CIFAR100 and, 20-Task CIFAR100. We found that, at the high sparsity level, uniform is a robust and better performer choice of initialization compared to ERK. Although the existing parameter isolation studies in continual learning [25, 26] have primarily employed uniform initialization, which aligns with our first finding, we also intriguingly find that ERK initialization exhibits good overall performance under low to moderate sparsity level (Figure 2, 3, 4, 5). In particular, uniform initialization saturates after 7 tasks, while the ERK initialization successfully completes all 10 tasks (Figure 3a, 3d and Figure 4a, 4d). The same phenomenon is also observed with 20-Task CIFAR100 where uniform initialization saturates after 7 tasks again, while the ERK initialization reaches this saturation after 13 tasks which indicates 85% efficient backbone usage (Figure 2a, 2d).

Table 1: Top-1 ACC (%), BWT (%), and FWT (%) scores of 20-Task CIFAR100.

sparsity	0.8			0.9			0.95		
	ACC	BWT	FWT	ACC	BWT	FWT	ACC	BWT	FWT
uniform									
random	52.70 ±17.86	0.01±0.28	14.74 ±3.78	69.91 ±5.05	<b>1.56 ±3.26</b>	<b>18.61 ±0.38</b>	74.96 ±5.81	<b>0.17 ±0.24</b>	18.52 ±0.98
unfired	46.67 ±18.03	<b>0.13 ±0.38</b>	13.53 ±3.93	69.44±5.63	-0.34 ±0.25	18.55 ±0.27	76.15 ±3.09	-0.10 ±0.36	18.73 ±0.55
gradient	47.71 ±7.30	-0.23 ±0.42	12.80 ±1.80	70.17 ±6.65	-0.73 ±0.24	18.02 ±1.17	<b>79.60 ±0.59</b>	0.07 ±0.37	<b>18.96 ±0.25</b>
momentum	50.01 ±11.12	0.18 ±0.36	13.58 ±2.92	70.97 ±6.08	0.04 ±0.33	18.23 ±0.67	79.12 ±0.97	-0.21 ±0.10	18.87 ±0.16
sparsity									
ERK									
random	<b>63.42 ±10.23</b>	-0.12 ±0.36	<b>14.87 ±1.93</b>	67.87 ±5.99	0.01 ±0.30	17.08 ±1.10	63.24 ±8.25	-0.26 ±0.29	18.27 ±1.10
unfired	61.97 ±14.02	-0.08 ±0.19	14.64 ±2.73	<b>66.51 ±6.92</b>	-0.19 ±0.08	16.74 ±1.13	65.74 ±12.41	-0.10 ±0.08	18.55 ±0.35
gradient	56.77 ±11.37	-0.13 ±0.12	13.23 ±2.69	<b>72.85 ±2.39</b>	0.01 ±0.65	17.50 ±0.79	74.23 ±1.92	0.01 ±0.35	18.72 ±0.15
momentum	60.35 ±11.12	-0.32 ±0.47	14.20 ±2.25	<b>73.57 ±1.96</b>	-0.05 ±0.62	17.81 ±0.32	75.07 ±1.94	0.08 ±0.13	18.81 ±0.26

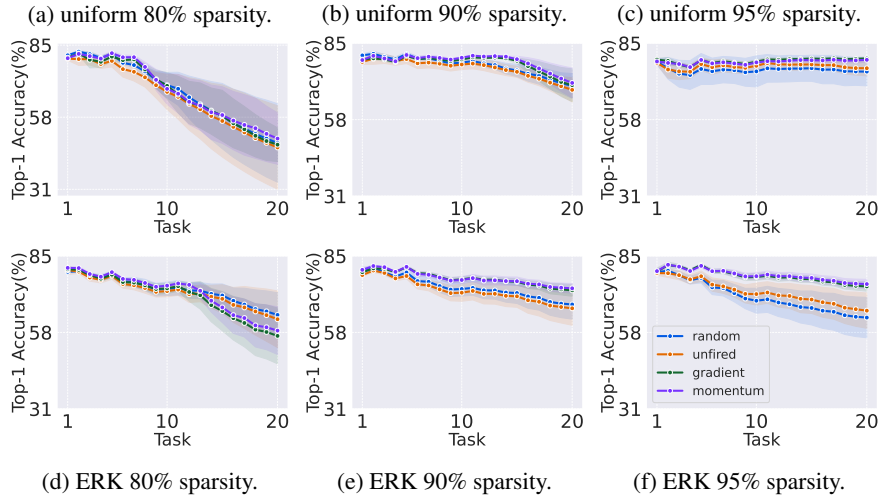


Figure 2: Top-1 ACC (%) of 20-Task CIFAR100 with different DST strategies. At a low to moderate sparsity, ERK utilizes the backbone more efficiently by using the connections within the narrow layers sparingly which allows to effectively learn longer increments of tasks and improves incremental performance: Uniform saturates after 7 tasks when sparsity level per task is 80%. ERK reaches this saturation after 13 tasks. At the high sparsity, however, uniform shows a more reliable and robust performance.

The reason behind this is the fact that uniform initialization creates a bottleneck within the narrow layers. We know that uniform initialization assigns equal connections to each layer without considering the layer size and ERK allocates more connections to the layers with more parameters and less connections to the layers with fewer parameters [28, 31]. Following a certain number of tasks, backbone’s capacity for sustaining the learning process is compromised since information flow through the backbone gets drastically decreased for the subsequent tasks. Our findings provide empirical support for the relationship between sparsity and information flow in CL setup: Specifically, in scenarios where the sparsity levels are high, we observe that information flow remains sustainable even with the uniform initialization. This suggests that the network retains sufficient connectivity to effectively accommodate new tasks. However, as the sparsity decreases, indicating a higher density of connections assigned per task, we observe a noticeable challenge in learning future tasks when backbone initialized uniformly. Therefore, under the same conditions, ERK initialization is better at protect information flow by using the connections within the narrow layers sparingly. Note that the reason to have these small BWT (%) scores is freezing all the connections except the batch normalization as we stated and discussed in the *Implementation Details*.

## 5.2. Growth strategy affects performance, tied to initialization and sparsity levels.

Our experimental results indicate that when the sparsity level is low, ERK initialization with random and unfired growth outperforms other alternatives (Table 1, 2, 3, 4). While the sparsity level is moderate, ERK and uniform initialization achieve similar performance where uniform initialization combined with gradient growth (uniform+gradient) tends to show a slightly better performance (Table 2, 3). In the case of extreme sparsity, the common approach of uniform+gradient [26] achieves noticeable performance while the ERK+gradient combination also demonstrates competitive results (Table 2, 3, 4). However, at an extreme sparsity level, the ERK+random and ERK+unfired exhibit lower accuracy performance (Table 1, 2, 3, 4). We also observe that uniform initialization is more resilient to the choice of growth strategies compared to ERK initialization (Figure 2, 3, 4, 5).

Overall, for the growth strategies in DST, gradient- and momentum-based growth provide better performance compared to random and unfired growth in the case of extreme sparsity yet random and unfired growth perform as good as gradient- and momentum-based growth in low-moderate sparsity. The rationale behind this is gradient and momentum-based methods are able to incorporate more information and can selectively add new connections between neurons that allow for faster exploration compared to random or unfired growth which needs more time to explore and find better connections.

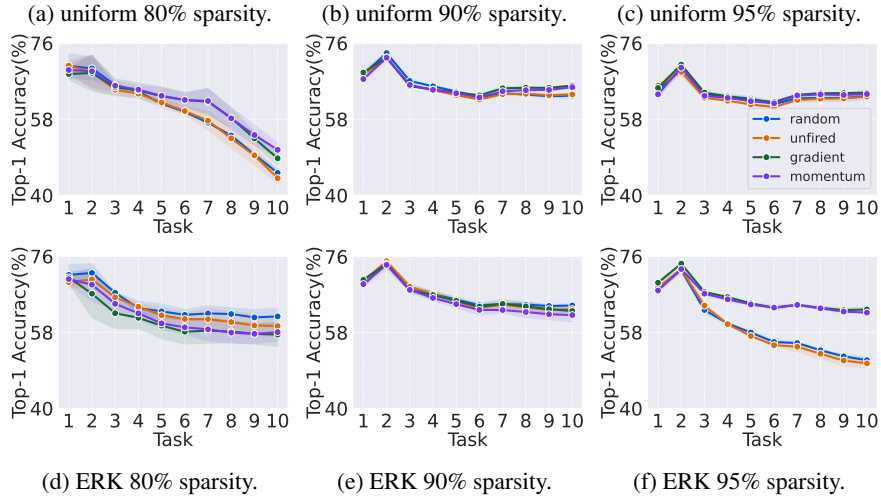


Figure 3: Top-1 ACC (%) of 10-Task miniImageNet with different DST criteria. ERK works still better at a low sparsity: Uniform saturates after 7 tasks while ERK successfully completes all tasks. In moderate sparsity, all DST approaches exhibit highly comparable performance. In the higher sparsity level, uniform emerges as a solid approach again but it is worth mentioning that ERK is able to perform nearly identical if right growth is selected.

Table 2: Top-1 ACC (%), BWT (%), and FWT (%) scores of 10-Task miniImageNet.

sparsity	0.8			0.9			0.95		
	ACC	BWT	FWT	ACC	BWT	FWT	ACC	BWT	FWT
uniform									
random	45.32 ±1.39	<b>0.42±0.67</b>	9.54 ±0.51	64.19 ±0.85	-0.08 ±0.08	9.38 ±0.34	63.43 ±1.01	-0.18 ±0.29	9.36 ±0.08
unfired	44.06 ±1.85	0.26 ±0.63	9.06 ±0.71	63.87±0.22	-0.29 ±0.81	9.47 ±0.16	63.35 ±0.04	-0.27 ±0.67	9.41 ±0.08
gradient	48.75 ±2.36	-0.05 ±0.06	8.57 ±0.44	<b>65.97 ±0.18</b>	0.11 ±0.47	<b>9.61 ±0.01</b>	<b>64.29 ±0.79</b>	-0.21 ±0.94	9.65 ±0.25
momentum	50.78 ±2.41	0.21 ±0.19	8.81 ±0.24	65.59 ±0.24	-0.48 ±0.11	9.39 ±0.03	63.96 ±0.71	0.15 ±0.24	9.29 ±0.11
sparsity									
ERK									
random	<b>61.78 ±2.72</b>	-0.25 ±0.65	<b>9.75 ±0.01</b>	64.41 ±0.46	0.26 ±0.44	9.54 ±0.13	51.43 ±1.07	<b>0.39 ±0.11</b>	<b>9.72 ±0.27</b>
unfired	59.49 ±3.21	-0.46 ±1.58	9.27 ±0.43	63.55 ±0.32	0.06 ±0.79	9.54 ±0.12	50.66 ±1.41	-0.22 ±0.41	9.22 ±0.41
gradient	57.47 ±3.01	0.15 ±0.73	8.31 ±0.48	63.12 ±1.38	0.05 ±0.23	9.28 ±0.17	63.47 ±0.68	-0.02 ±0.22	9.38 ±0.01
momentum	58.06 ±3.98	-0.46 ±0.44	8.39 ±0.34	62.15 ±2.25	<b>0.36 ±0.02</b>	8.78 ±0.38	62.68 ±0.46	0.37 ±0.19	9.16 ±0.25

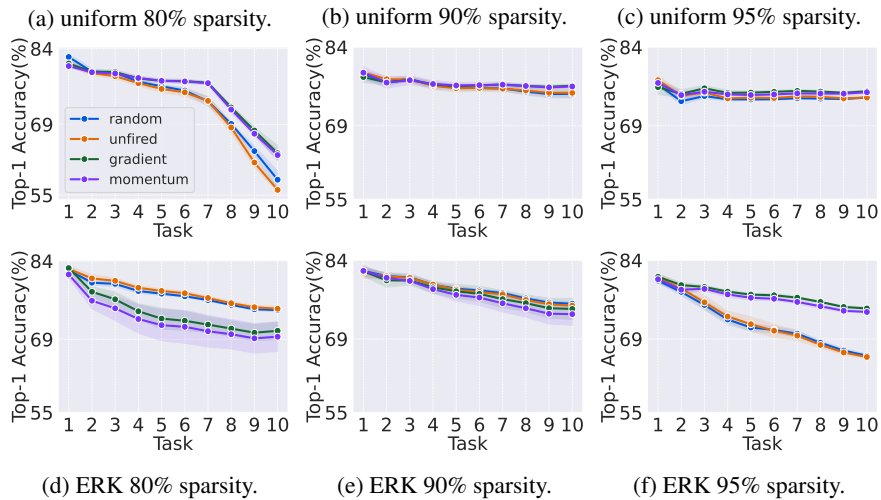


Figure 4: Top-1 ACC (%) of 10-Task CIFAR100 with different DST criteria. Findings align with the 10-Task miniImageNet.

Table 3: Top-1 ACC (%), BWT (%), and FWT (%) scores of 10-Task CIFAR100.

sparsity	0.80			0.90			0.95		
	ACC	BWT	FWT	ACC	BWT	FWT	ACC	BWT	FWT
uniform									
random	58.04 ±1.96	-0.03 ±0.26	9.03 ±0.27	75.09 ±0.91	-0.13 ±0.56	9.35 ±0.16	74.39 ±0.17	-0.02 ±0.22	8.97 ±0.23
unfired	56.03 ±0.57	-0.16 ±0.18	8.41 ±0.29	75.28 ±0.94	0.025 ±0.27	9.27 ±0.15	74.38 ±0.22	-0.10 ±0.09	9.22 ±0.21
gradient	63.29 ±1.72	0.002 ±0.03	9.06 ±0.19	<b>76.63 ±0.41</b>	-0.11 ±0.17	9.49 ±0.12	<b>75.57 ±0.21</b>	-0.19 ±0.16	<b>9.56 ±0.09</b>
momentum	62.92 ±1.12	0.03 ±0.19	8.94 ±0.09	76.49 ±0.26	<b>0.11 ±0.30</b>	9.26 ±0.23	75.40 ±0.44	-0.07 ±0.32	9.18 ±0.12
sparsity									
ERK									
random	74.61 ±0.44	-0.05 ±0.22	9.52 ±0.24	75.71 ±0.32	-0.06 ±0.11	<b>9.68 ±0.25</b>	65.81 ±0.37	<b>-0.01 ±0.36</b>	9.49 ±0.12
unfired	<b>74.86 ±0.54</b>	0.025 ±0.41	<b>9.52 ±0.22</b>	75.33 ±0.33	-0.06 ±0.07	9.64 ±0.14	65.56 ±0.49	-0.16 ±0.24	9.46 ±0.29
gradient	70.63 ±1.91	<b>0.14 ±0.31</b>	7.91 ±0.28	74.71 ±2.33	0.01 ±0.42	8.68 ±0.14	74.81 ±0.37	-0.04 ±0.25	8.97 ±0.13
momentum	69.51 ±3.26	-0.29 ±0.25	7.57 ±0.55	73.73 ±2.43	0.02 ±0.31	8.21 ±0.74	74.14 ±0.22	-0.03 ±0.25	8.44 ±0.13

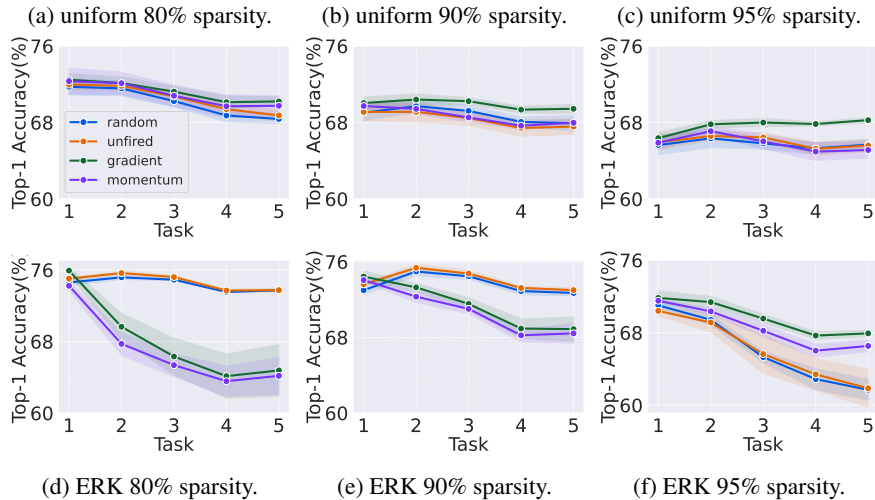


Figure 5: Top-1 ACC (%) of 5-Task CIFAR100 with various DST strategies. Interestingly, findings align with 20-Task CIFAR100: ERK improves incremental accuracy at a low to moderate sparsity. On the other hand, at the high sparsity, uniform appears as a more reliable strategy yet ERK is able to perform nearly identical if right growth is selected.

Table 4: Top-1 ACC (%), BWT (%), and FWT (%) scores of 5-Task CIFAR100.

sparsity	0.80			0.90			0.95		
	ACC	BWT	FWT	ACC	BWT	FWT	ACC	BWT	FWT
uniform									
random	68.37 ±0.58	-0.16 ±0.09	4.54 ±0.09	67.92 ±0.93	0.04 ±0.23	4.36 ±0.19	65.68 ±0.62	0.01 ±0.12	4.33 ±0.11
unfired	68.79 ±0.71	<b>0.13 ±0.33</b>	4.53 ±0.18	67.57 ±0.93	0.04 ±0.28	4.42 ±0.11	65.69 ±0.72	<b>0.15 ±0.33</b>	4.35 ±0.29
gradient	70.21 ±0.55	-0.36 ±0.51	4.74 ±0.21	69.43 ±0.52	0.17 ±0.17	4.86 ±0.23	<b>68.25 ±0.31</b>	0.05 ±0.33	<b>5.12 ±0.18</b>
momentum	69.75 ±1.23	-0.025 ±0.32	4.46 ±0.22	67.93 ±0.46	-0.14 ±0.16	4.21 ±0.13	65.12 ±0.97	-0.24 ±0.14	4.15 ±0.41
sparsity									
ERK									
random	73.72 ±0.09	-0.16 ±0.36	5.19 ±0.21	72.7 ±0.33	-0.13 ±0.29	5.13 ±0.05	61.7 ±1.32	-0.22 ±0.26	4.36 ±0.39
unfired	<b>73.73 ±0.27</b>	0.03 ±0.11	<b>5.34 ±0.21</b>	<b>73.01 ±0.27</b>	<b>0.18 ±0.08</b>	<b>5.17 ±0.17</b>	61.86 ±2.41	-0.11 ±0.31	4.11 ±0.35
gradient	64.76 ±3.34	-0.12 ±0.33	3.58 ±0.26	68.87 ±1.47	0.02 ±0.25	3.85 ±0.03	67.92 ±0.38	-0.08 ±0.24	3.66 ±0.14
momentum	64.16 ±2.37	-0.14 ±0.19	3.51 ±0.14	68.43 ±1.17	-0.01 ±0.31	3.45 ±0.09	66.53 ±0.73	0.06 ±0.22	3.23 ±0.14

### 5.3. Adaptivity improves performance since there is no panacea.

Throughout our experiments, we have observed that there is no universally successful approach in terms of different task numbers and sparsity levels. When the number of tasks is high, the choice of both initialization and growth strategies become crucial, depending on the sparsity level. It is unlikely to exist a panacea DST setup for all datasets or tasks, and it is not feasible to try different alternatives for each scenario due to computational cost and time. Therefore, we hypothesized that an adaptive approach for selecting DST criteria per task should improve the performance.

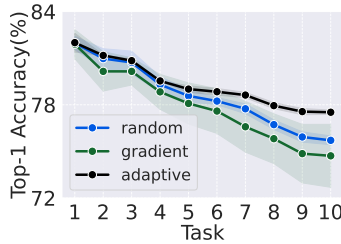


Figure 6: Adaptive growth strategy on 10-task CIFAR100 scenario. Adaptive approach outperforms the fixed strategy.

In our final experiment, we construct a naive adaptive growth strategy with ERK initialization to validate our hypothesis, wherein random growth is implemented for the first five tasks, and gradient growth is selected for the subsequent five tasks while sparsity per task is 90% on the 10-task CIFAR100 dataset. The adaptive approach yields better performance when compared to two baselines which are pre-selected and fixed growth strategies of random and gradient with ERK initialization (Figure 6). This is because of that during the initial stage of learning, there exists considerable potential for exploration of the model parameters. Therefore, a random growth strategy tends to be more efficient and effective when the exploration space is sufficiently large. However, as the model capacity becomes more saturated, the gradient growth strategy becomes increasingly effective and superior to random growth which results in better overall performance.

## 6. Discussion

**Conclusion.** This paper has presented a comprehensive analysis, aiming to evaluate different components of Dynamic Sparse Training in Continual Learning. We focus on the Parameter Isolation strategy to find the best subnetwork for each task under various conditions that highly affect the final topologies. Through large-scale experiments, we found that choice of sparsity level, initialization, and growth strategy significantly affects the incremental performance. In our findings, when sparsity is low, Erdős-Rényi Kernel (ERK) initialization exploits the backbone efficiently, enabling the learning continually. However, as sparsity increases, uniform initialization demonstrates more consistent and stable performance. The performance of the growth strategy relies on the chosen initialization method and the level of sparsity. As a final observation, even naive adaptive selection for DST criteria per task improves the incremental performance compared to using fixed and pre-defined strategies for all tasks. We hope empirical results that are found in this study inspire the community to make informed decisions regarding the applicability of these strategies in real-world scenarios and pave the way for future studies in this domain.

**Limitations and Future Work.** To extend the scope of this study, structured dynamic sparse training should also be analyzed to grasp the underlying mechanism of dynamic sparse training comprehensively in continual learning. Finally, the observed performance improvements in incremental learning are significant with a simple adaptive approach. Therefore, further investigation on more sophisticated adaptive DST strategies promises a highly promising research direction.

## References

- [1] James Kirkpatrick, Razvan Pascanu, Neil Rabinowitz, Joel Veness, Guillaume Desjardins, Andrei A Rusu, Kieran Milan, John Quan, Tiago Ramalho, Agnieszka Grabska-Barwinska, et al. Overcoming catastrophic forgetting in neural networks. *PNAS*, 2017.
- [2] Zhizhong Li and Derek Hoiem. Learning without forgetting. *TPAMI*, 2017.
- [3] Friedemann Zenke, Ben Poole, and Surya Ganguli. Continual learning through synaptic intelligence. In *ICML*, 2017.
- [4] Saihui Hou, Xinyu Pan, Chen Change Loy, Zilei Wang, and Dahua Lin. Lifelong learning via progressive distillation and retrospection. In *ECCV*, 2018.
- [5] Minsoo Kang, Jaeyoo Park, and Bohyung Han. Class-incremental learning by knowledge distillation with adaptive feature consolidation. In *CVPR*, 2022.
- [6] Sylvestre-Alvise Rebuffi, Alexander Kolesnikov, Georg Sperl, and Christoph H Lampert. icarl: Incremental classifier and representation learning. In *CVPR*, 2017.
- [7] David Lopez-Paz and Marc’Aurelio Ranzato. Gradient episodic memory for continual learning. In *NeurIPS*, 2017.

- [8] Yaoyao Liu, Qianru Sun, and Qianru Sun. Rmm: Reinforced memory management for class-incremental learning. In *NeurIPS*, 2021.
- [9] Decebal Constantin Mocanu, Maria Torres Vega, Eric Eaton, Peter Stone, and Antonio Liotta. Online contrastive divergence with generative replay: Experience replay without storing data. *arXiv preprint arXiv:1610.05555*, 2016.
- [10] Hanul Shin, Jung Kwon Lee, Jaehong Kim, and Jiwon Kim. Continual learning with deep generative replay. In *NeurIPS*, 2017.
- [11] Wenpeng Hu, Zhou Lin, Bing Liu, Chongyang Tao, Zhengwei Tao Tao, Dongyan Zhao, Jinwen Ma, and Rui Yan. Overcoming catastrophic forgetting for continual learning via model adaptation. In *ICLR*, 2019.
- [12] Chen He, Ruiping Wang, Shiguang Shan, and Xilin Chen. Exemplar-supported generative reproduction for class incremental learning. In *BMVC*, 2018.
- [13] Shipeng Yan, Jiangwei Xie, and Xuming He. Der: Dynamically expandable representation for class incremental learning. In *CVPR*, 2021.
- [14] Fu-Yun Wang, Da-Wei Zhou, Han-Jia Ye, and De-Chuan Zhan. Foster: Feature boosting and compression for class-incremental learning. In *ECCV*, 2022.
- [15] Da-Wei Zhou, Qi-Wei Wang, Han-Jia Ye, and De-Chuan Zhan. A model or 603 exemplars: Towards memory-efficient class-incremental learning. In *ICLR*, 2023.
- [16] Quang Pham, Chenghao Liu, and Steven Hoi. Dualnet: Continual learning, fast and slow. In *NeurIPS*, 2021.
- [17] Rahaf Aljundi, Punarjay Chakravarty, and Tinne Tuytelaars. Expert gate: Lifelong learning with a network of experts. In *CVPR*, 2017.
- [18] Mitchell Wortsman, Vivek Ramanujan, Rosanne Liu, Aniruddha Kembhavi, Mohammad Rastegari, Jason Yosinski, and Ali Farhadi. Supermasks in superposition. In *NeurIPS*, 2020.
- [19] Arun Mallya, Dillon Davis, and Svetlana Lazebnik. Piggyback: Adapting a single network to multiple tasks by learning to mask weights. In *ECCV*, 2018.
- [20] Siavash Golkar, Michael Kagan, and Kyunghyun Cho. Continual learning via neural pruning. In *NeurIPS*, 2019.
- [21] Aleksandr Dekhovich, David MJ Tax, Marcel HF Sluiter, and Miguel A Bessa. Continual prune-and-select: class-incremental learning with specialized subnetworks. *Applied Intelligence*, 2023.
- [22] Arun Mallya and Svetlana Lazebnik. Packnet: Adding multiple tasks to a single network by iterative pruning. In *CVPR*, 2018.
- [23] Ghada Sokar, Decebal Constantin Mocanu, and Mykola Pechenizkiy. Spacenet: Make free space for continual learning. *Neurocomputing*, 2021.
- [24] Ghada Sokar, Decebal Constantin Mocanu, and Mykola Pechenizkiy. Avoiding forgetting and allowing forward transfer in continual learning via sparse networks. In *ECML PKDD*. Springer, 2023.
- [25] Mustafa Burak Gurbuz and Constantine Dovrolis. Nispa: Neuro-inspired stability-plasticity adaptation for continual learning in sparse networks. In *ICML*, 2022.
- [26] Haeyong Kang, Rusty John Lloyd Mina, Sultan Rizky Hikmawan Madjid, Jaehong Yoon, Mark Hasegawa-Johnson, Sung Ju Hwang, and Chang D Yoo. Forget-free continual learning with winning subnetworks. In *ICML*, 2022.
- [27] Zifeng Wang, Zheng Zhan, Yifan Gong, Geng Yuan, Wei Niu, Tong Jian, Bin Ren, Stratis Ioannidis, Yanzhi Wang, and Jennifer Dy. Sparcl: Sparse continual learning on the edge. In *NeurIPS*, 2022.

- [28] Decebal Constantin Mocanu, Elena Mocanu, Peter Stone, Phuong H Nguyen, Madeleine Gibescu, and Antonio Liotta. Scalable training of artificial neural networks with adaptive sparse connectivity inspired by network science. *Nature communications*, 2018.
- [29] Shiwei Liu and Zhangyang Wang. Ten lessons we have learned in the new "sparseland": A short handbook for sparse neural network researchers. *arXiv preprint arXiv:2302.02596*, 2023.
- [30] Torsten Hoefer, Dan Alistarh, Tal Ben-Nun, Nikoli Dryden, and Alexandra Peste. Sparsity in deep learning: Pruning and growth for efficient inference and training in neural networks. *JMLR*, 2021.
- [31] Utku Evci, Trevor Gale, Jacob Menick, Pablo Samuel Castro, and Erich Elsen. Rigging the lottery: Making all tickets winners. In *ICML*, 2020.
- [32] Tim Dettmers and Luke Zettlemoyer. Sparse networks from scratch: Faster training without losing performance. *arXiv preprint arXiv:1907.04840*, 2019.
- [33] Siddhant Jayakumar, Razvan Pascanu, Jack Rae, Simon Osindero, and Erich Elsen. Top-kast: Top-k always sparse training. In *NeurIPS*, 2020.
- [34] Shiwei Liu, Lu Yin, Decebal Constantin Mocanu, and Mykola Pechenizkiy. Do we actually need dense over-parameterization? in-time over-parameterization in sparse training. In *ICML*, 2021.
- [35] Shiwei Liu, Tim Van der Lee, Anil Yaman, Zahra Atashgahi, Davide Ferraro, Ghada Sokar, Mykola Pechenizkiy, and Decebal Constantin Mocanu. Topological insights into sparse neural networks. In *ECML PKDD*, 2021.
- [36] Tianlong Chen, Zhenyu Zhang, Sijia Liu, Shiyu Chang, and Zhangyang Wang. Long live the lottery: The existence of winning tickets in lifelong learning. In *ICLR*, 2021.
- [37] Yann LeCun, John Denker, and Sara Solla. Optimal brain damage. In *NeurIPS*, 1989.
- [38] Alex Krizhevsky, Geoffrey Hinton, et al. Learning multiple layers of features from tiny images. 2009.
- [39] Oriol Vinyals, Charles Blundell, Timothy Lillicrap, Koray Kavukcuoglu, and Daan Wierstra. Matching networks for one shot learning. In *NeurIPS*, 2016.
- [40] Natalia Díaz-Rodríguez, Vincenzo Lomonaco, David Filliat, and Davide Maltoni. Don't forget, there is more than forgetting: new metrics for continual learning. *arXiv preprint arXiv:1810.13166*, 2018.
- [41] Adam Paszke, Sam Gross, Francisco Massa, Adam Lerer, James Bradbury, Gregory Chanan, Trevor Killeen, Zeming Lin, Natalia Gimelshein, Luca Antiga, Alban Desmaison, Andreas Kopf, Edward Yang, Zachary DeVito, Martin Raison, Alykhan Tejani, Sasank Chilamkurthy, Benoit Steiner, Lu Fang, Junjie Bai, and Soumith Chintala. Pytorch: An imperative style, high-performance deep learning library. In *NeurIPS*. 2019.
- [42] Kaiming He, Xiangyu Zhang, Shaoqing Ren, and Jian Sun. Deep residual learning for image recognition. In *CVPR*, 2016.